

Strong-field double ionization at the transition to below the recollision thresholdD. F. Ye^{1,2,3} and J. Liu^{1,3,*}¹*Institute of Applied Physics and Computational Mathematics, Beijing 100088, People's Republic of China*²*Graduate School, China Academy of Engineering Physics, Beijing 100088, People's Republic of China*³*Center for Applied Physics and Technology, Peking University, Beijing 100084, People's Republic of China*

(Received 28 September 2009; published 8 April 2010)

We investigate the strong-field double ionization using a semiclassical model, in which the recollision-induced excitation-tunneling (RIET) effect has been taken into account with the Wentzel-Kramers-Brillouin (WKB) approach. When the laser intensity is below the recollision threshold, we find that both RIET and multiple recollisions become significant and can produce the anticorrelated (back-to-back) electron pair. Distinct footprints left by these two mechanisms on the correlated momentum spectra have been identified. As another signature of the transition to below the recollision threshold regime, we find that the V-shaped (or fingerlike) structure in the correlated momentum spectra fades away. Our model calculations have been compared with a recent experiment on argon atoms.

DOI: [10.1103/PhysRevA.81.043402](https://doi.org/10.1103/PhysRevA.81.043402)

PACS number(s): 32.80.Fb, 33.80.Rv, 42.50.Hz

I. INTRODUCTION

During the past decades, experiments on strong-field double ionization (DI) have constantly exhibited surprising data that challenge our existing knowledge. At first, the distinguished knee structure on the ionization curve revealed that the production of doubly charged ions could be enhanced by several orders of magnitude in comparison with the prediction of independent-electron models [1]. It is natural to imagine that electron-electron correlation is responsible for the observed discrepancy. However, there has been a longstanding debate on how the two electrons correlate in practice [2–4]. The puzzle is being resolved step by step with the help of cold target recoil ion momentum spectroscopy (COLTRIMS). It was clearly shown that the two electrons have a greater probability of being emitted in the same direction parallel to the laser polarization [5], meanwhile leaving a footprint on the ion momentum distribution with a double-hump structure [6]. Recently, with the advances in high-resolution coincidence techniques, two experimental groups revisited the correlated momentum spectra and amazingly found a never observed (at that time) V-shaped (or fingerlike) structure, which is claimed as the signature of backscattering [7]. All these characteristic features together elect rescattering out of numerous possible mechanisms as the dominant contribution to the enhanced double ionization yield.

In the rescattering picture, one electron is first released through quantum tunneling, then is driven back to its parent ion and imparts its kinetic energy to dislodge a second electron [3]. The maximal energy of the returned electron is $3.17U_p$ [where $U_p = \epsilon_0^2/(4\omega^2)$ is the ponderomotive energy with electric field amplitude ϵ_0 and laser frequency ω]. When the idea of recollision was first introduced, it was anticipated that the double ionization yield would undergo a sudden drop supposing the maximum returned energy is smaller than the ionization potential of the inner electron, that is, in the regime below the recollision threshold (BRT). But, by now it is widely recognized that recollision excitation and field suppression

effects might extend the process to lower intensities. More interestingly, a recent experiment in the deep BRT regime [8] has revealed that the two photoelectrons most often drift out in opposite directions, showing the so-called anticorrelated phenomenon, in contrast to all previous observations near or above the recollision threshold (see, for example, Refs. [5,7]). A comprehensive understanding of the physical origin of this striking phenomena is far from complete, although some progress has been made toward the BRT regime using both a purely classical approach [9] and a quantum treatment [10].

In the present paper, we investigate the strong-field double ionization at the transition to the BRT regime using a recently developed semiclassical model, in which the recollision-induced excitation-tunneling (RIET) effect has been taken into account with the Wentzel-Kramers-Brillouin (WKB) approach. In the BRT regime, since the energy of the returned electron is relatively small, the RIET effect becomes important. Therefore, this extension is crucial. With this semiclassical model, we are capable of reproducing the transition from correlation to anticorrelation as the laser intensity decreases to the deep BRT regime, in accordance with the recent experiment on argon atoms. We identify that both RIET and multiple recollisions are responsible for the transition and these two mechanisms are found to leave distinct footprints on the correlated momentum spectra. As another signature of the transition, we find that the V-shaped structure in the correlated momentum spectra completely fades away.

Our paper is organized as follows. In Sec. II, we present our model. Section III gives our main results. Finally, we provide some further discussion and draw a conclusion in Sec. IV.

II. MODEL

We consider a two-active-electron atom interacting with an infrared laser pulse. One electron is released at the outer edge of the field-suppressed Coulomb barrier through quantum tunneling with a rate given by the ADK formula [11]. The tunneled electron has a Gaussian-like distribution for the

*liu_jie@iapcm.ac.cn

transverse velocity and zero longitudinal velocity [12]. The bound electron is sampled from a microcanonical distribution [13]. The subsequent evolution of the two electrons with these initial conditions is governed by Newton's equations of motion: $\frac{d^2 \mathbf{r}_i}{dt^2} = -\epsilon(t) - \nabla_{\mathbf{r}_i} (V_{ne}^i + V_{ee})$. Here, index i denotes the two different electrons. $V_{ne}^i = -\frac{2}{|\mathbf{r}_i|}$ and $V_{ee} = \frac{1}{|\mathbf{r}_1 - \mathbf{r}_2|}$ are Coulomb interactions between nucleus and electrons and between two electrons, respectively. The laser field $\epsilon(t)$ has a constant amplitude for the first ten cycles and is turned off with a three-cycle ramp.

This model has been proven to work well in the regime above the recollision threshold [12]. To extend it to the BRT regime, we need to include the RIET effect in the second step. This is done by allowing the bound electron to tunnel through the potential barrier whenever it reaches the outer turning point, where $p_{i,z} = 0$ and $z_i \epsilon(t) < 0$, with a tunneling probability P_i^{tun} given by the WKB approximation

$$P_i^{\text{tun}} = \exp \left[-2\sqrt{2} \int_{z_i^{\text{in}}}^{z_i^{\text{out}}} \sqrt{V(z_i) - V(z_i^{\text{in}})} dz_i \right]. \quad (1)$$

Here, z_i^{in} and z_i^{out} are the two roots ($|z_i^{\text{out}}| > |z_i^{\text{in}}|$) of the equation for z_i and $V(z_i) = -2/r_i + z_i \epsilon(t) = -2/r_i^{\text{in}} + z_i^{\text{in}} \epsilon(t)$ [14].

This two-electron system is solved by employing the standard fourth- to fifth-order Runge-Kutta algorithm, and DI events are identified by an energy criterion. In our calculations, the first and second ionization potentials of the two-electron atom are chosen as $I_{p1} = -0.58$ a.u. and $I_{p2} = -1.02$ a.u., respectively, to match the experimental data for the argon atom. The laser frequency is $\omega = 0.057$ a.u., corresponding to a wavelength of 800 nm. More than 10^7 weighted (i.e., by the tunneling rate) classical two-electron trajectories are traced until $13T$ to obtain the distribution of correlated momentum, where T is the oscillating period of the laser field. Finally, more than 10^4 DI events are collected for statistics. Numerical convergence has been tested by increasing the number of trajectories twice.

Before presenting our main results, we need to make some remarks on this model: (i) In our consideration, the atom is essentially helium-like. To extend it to include the shielding effect from the inner shell electrons, one may replace the nuclear Coulomb-type potential with a structural Hartree-Fock-type effective interaction potential as given in Ref. [15]. This shielding effect is an interesting issue for future study. (ii) In our model, the nonsequential DI (NSDI) dynamics is accomplished through either quantum tunneling or classical over-the-barrier ionization, whereas the multiphoton ionization effect is ignored. For the lowest laser intensity in our following calculations, the Keldysh parameter [16] $\gamma = \sqrt{|I_{p1}|/2U_p} = 1.8$. In this case, the multiphoton effect may play a role to some extent. However, recent classical calculations that involve only over-the-barrier ionization has reproduced well some of the experimental observations under relevant laser parameters, thus indicating that the multiphoton effect is not so important for the case we consider [9,17].

III. MAIN RESULTS

A. Double ionization at the transition to below the recollision threshold

We have calculated the correlated momentum spectra with this semiclassical model for a broad range of laser intensities. The statistics on the momentum distribution for all DI events at three different laser intensities, $I = 2 \times 10^{14}$ W/cm² (high), 9×10^{13} W/cm² (moderate), and 4×10^{13} W/cm² (low), are presented in the first column of Fig. 1. A simple estimation of the intensity threshold is given by $3.17U_p = |I_{p2}|$, which gives 1.5×10^{14} W/cm². So, for the lowest laser intensity, the system has fallen deep into the BRT regime.

Our calculations have reproduced many key features observed in the experiments. At the highest laser intensity, the spectrum presents a correlated behavior, that is, the electron pairs have a higher probability of being emitted in the same direction parallel to the laser polarization. Moreover, the distribution exhibits an overall V-shaped structure, as found independently by two experimental groups at the end of 2007 [7]. Theoretical interpretation of these characters has been advanced by many theoretical calculations [18–22]. With the help of classical trajectory diagnosis, the distinct roles of the nuclear Coulomb attraction and the electron-electron Coulomb repulsion in forming the V-shaped structure have been identified for NSDI events provoked by single recollision [20].

The momentum distribution becomes quite different as the laser intensity decreases. For moderate laser intensity, two red spots (high probability) start to appear in the second and fourth quadrants and the V-shaped structure in the first and third quadrants starts to fade away. When the intensity decreases deep into the BRT regime, the V-shaped structure totally disappears and the distribution tends to align along the anticorrelated diagonal of $p_1^{\parallel} = -p_2^{\parallel}$. These results are consistent with recent experimental observations [8]. With the simulations, we have demonstrated a clear transition from correlation to anticorrelation and the disappearance of the V-shaped structure in the deep BRT regime. These significant changes on the momentum distribution presumably reflect the variation of the underlying mechanisms leading to NSDI.

It is well known that when the tunneled electron is thrown back to the parent core, its maximal kinetic energy is $3.17U_p$. As the laser intensity gradually decreases, the maximal recolliding energy becomes insufficient to directly ionize the inner electron. This is the case for the lowest laser intensity in these calculations, where $3.17U_p = 0.28$ a.u. is far below $|I_{p2}| = 1.02$ a.u.. As one may expect, the inner electron that has been excited by the first recollision requires other mechanisms to liberate it, for example, by means of a second (even multiple) recollision or field-assisted tunneling ionization. It is straightforward to model the former classically [9]. We term it as the recollision-induced direct ionization (RIDDI). The latter, that is, the recollision-induced excitation tunneling, is of quantum nature and beyond the capability of previous classical treatments [9]. These two different mechanisms leave distinct footprints in the correlated momentum spectra. This can be clearly seen by comparing the second and third columns of Fig. 1, where we split the total correlated momentum spectra into two parts according to different emission mechanisms.

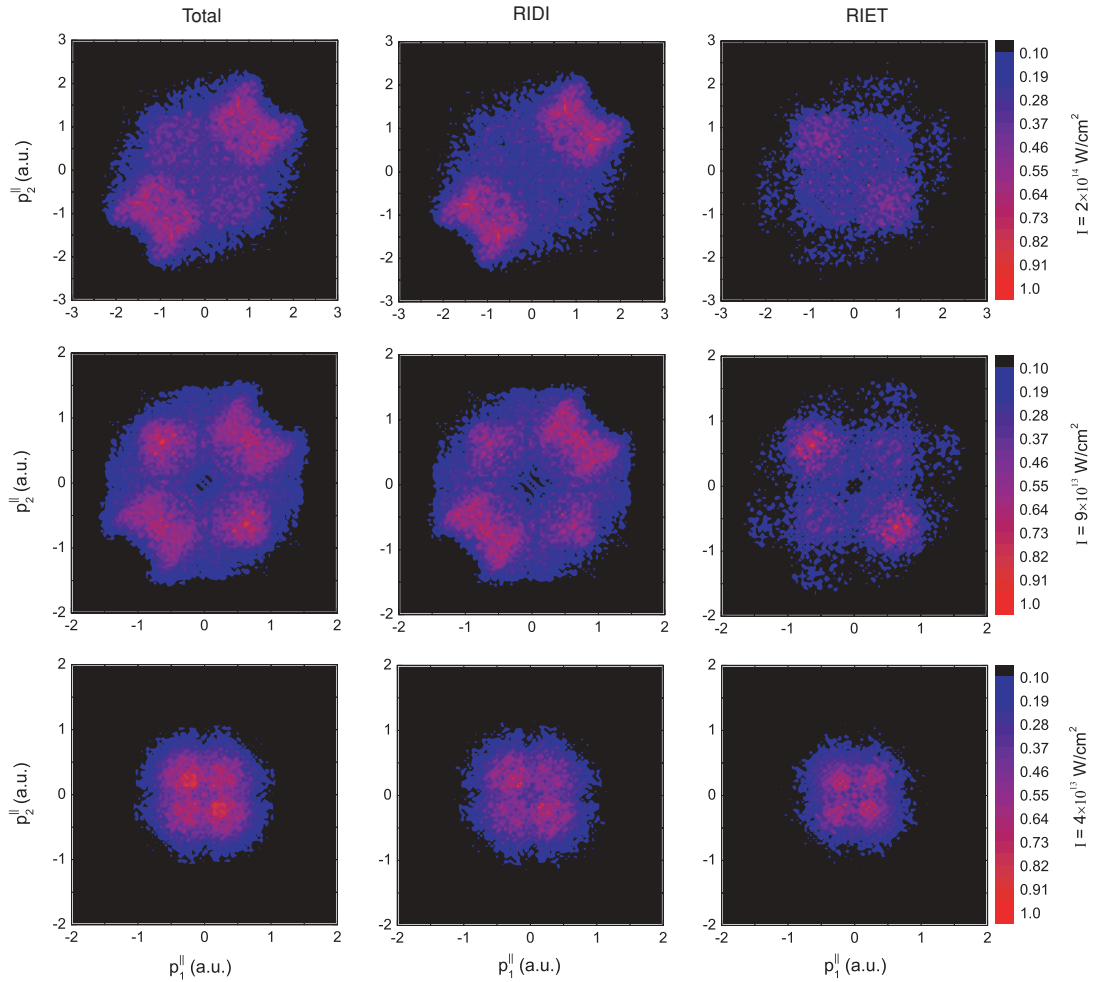


FIG. 1. (Color online) Correlated momentum spectra for double ionization of argon at different laser intensities ranging from above to below the recollision threshold. Shown are the momentum components $p_{1,2}^{\parallel}$ along the laser polarization direction. The second and third columns are deduced from the first column by superimposing additional restrictions on our statistics according to different emission mechanisms. See text for details.

From the middle column of Fig. 1 for the RIDI mechanism, we see that the correlated momentum spectra exhibit a clear transition from the dominance of correlated emission to a situation where anticorrelated ejection has become much stronger and even the most important contribution, when the laser intensity decreases to the BRT regime. The patterns are to some extent analogous to that in the first column for the total distribution.

We plot two typical trajectories, corresponding to the single-recollision-induced correlated emission and double-recollision-induced anticorrelated emission, in Figs. 2(a) and 2(d) and 2(b) and 2(e), respectively.

In Fig. 2(a) and 2(d), the returned electron possesses high incident kinetic energy, thus a single recollision is enough to “kick out” the inner electron within half a cycle and push it to move along the recolliding direction. Then the laser field quickly reverses the struck electron, and finally both electrons drift out in the backward direction, with one following the other. This configuration usually emerges in the higher intensity regime. The “time delay” between the recollision and double ionization is less than 1/4 optical cycle [i.e., one optical cycle (o.c.) ~ 2.67 fs].

The “time delay” picture is very helpful for understanding the correlated dynamics at high laser intensities [23,24]. There, the time delay is defined as the time lag between the recollision (i.e., the moment when two electrons become closest) and the double ionization (i.e., the moment when both electrons’ energies become greater than zero [23]). In Ref. [24], it was found that two photoelectrons are alternately emitted into the same hemisphere and opposite hemispheres as the time delay increases from odd half-cycles to even half-cycles and repeats again. This picture is also applicable to our cases of higher intensities (i.e., $I = 2 \times 10^{14}$ and $I = 9 \times 10^{13}$ W/cm²), where single-recollision-induced DI dominates as presented in Figs. 2(a) and 2(d).

However, in the deep BRT regime (e.g., $I = 4 \times 10^{13}$ W/cm²), the recollision process is more complex because of the multiple collisions and chaotic motions involved [25–27]. In this regime, our calculation shows no clear correspondence between the time delay and the emission hemisphere. We thus modify the concept of time delay as the time lag between the ionization moment of the first electron and the moment of double ionization. When we compile statistics on the quadrant distribution according to

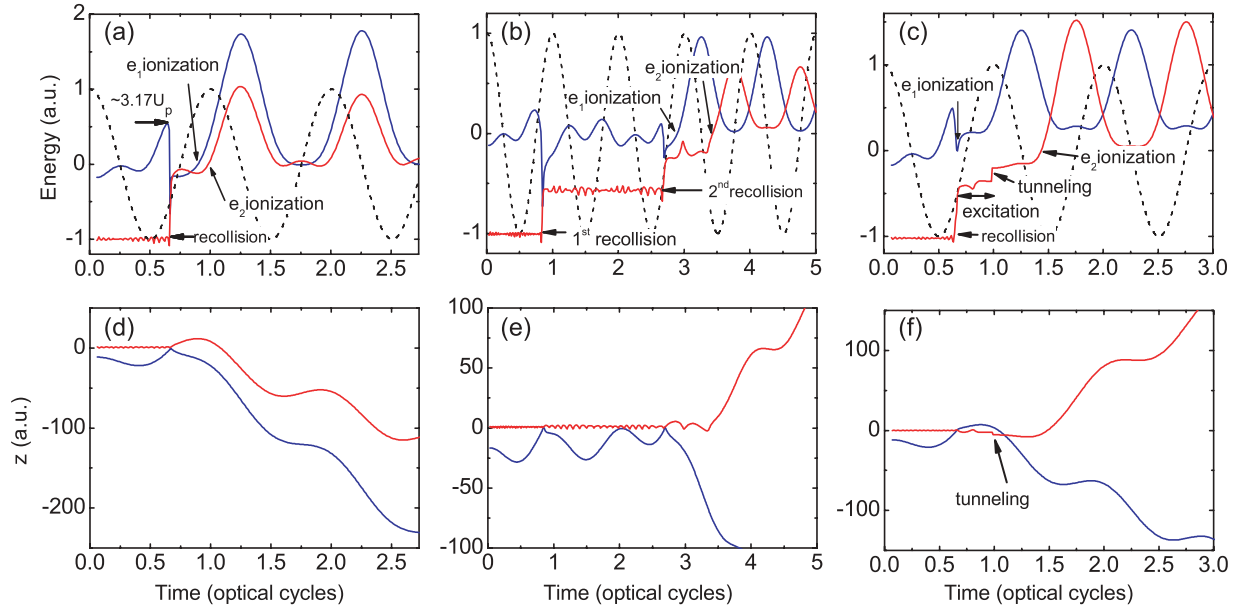


FIG. 2. (Color online) Typical trajectories for NSDI: (a) Double ionization is induced directly by single recollision and by means of (b) two recollisions or (c) recollision-induced excitation-tunneling. (d)–(f) show the coordinate evolution of the two electrons along the laser field direction. The blue (dark gray) and red (light gray) curves, respectively, denote the tunneled electron and the inner one. The black dashed curves in (a)–(c) represent the laser electric field. Note that there is no collision at $t = 2.0$ o.c. in (e) and $t = 1.15$ o.c. in (f). In both cases, the distance in the lateral direction is very large. In (f) a small displacement along z toward negative values is just discernible as a result of the tunneling labeled by an arrow, placing the “classical” electron abruptly at a different position; see text for details.

the newly defined “time delay,” a strong correlation has been observed [28]. With this, the time delay scenario applies to intensities ranging from above threshold to the deep BRT regime. Notice that, for the case of higher intensity, the newly defined “time delay” is equivalent to the old one, because the the first recollision is strong so that the first electron is ionized almost simultaneously at the recollision moment.

At low laser intensities, a second recollision is required to liberate the inner electron, as demonstrated explicitly by the classical trajectories in Figs. 2(b) and 2(e). Here, the opposite-hemisphere ionizations hinge on having a time delay of $\sim 1/2$ o.c. between the ionization moment of the first electron and the second one. During the $1/2$ cycle, the field has reversed its direction, leading to back-to-back emission of the electrons. Physically, at low intensities the second recollision usually is weak; after the second recollision, both electrons still populate bound states. The strong $e-e$ repulsion will push one electron to pass over the Coulomb barrier at the first coming field maximum, while leaving the other one being hindered until the second field maximum [see Figs. 2(b) and 2(e)]. A similar mechanism was also discussed in Ref. [9].

The transition from correlation to anticorrelation, however, obviously, cannot be demarcated by $3.17U_p = |I_{p2}|$. For a moderate laser intensity of 9×10^{13} W/cm² where $3.17U_p = 0.63$ a.u. is obviously below $|I_{p2}| = 1.02$ a.u., the momentum distribution still mainly occupies the first and third quadrants and presents an obscure V-shaped structure. We carefully checked the individual classical trajectories for this case and found that double ionization is still mainly provoked by single recollision as demonstrated in Figs. 2(a) and 2(d).

For the RIET mechanism, its percentage over the total double ionization events increases from 23.07% at $2 \times$

10^{14} W/cm² to 32.79% at 4×10^{13} W/cm². We find amazingly that NSDI events caused by this mechanism always have a greater probability of occupying the second and fourth quadrants in the correlated momentum plane, no matter whether the laser intensity is below or above the recollision threshold. The percentage of doubly ionizing trajectories in these two quadrants is always beyond 50%, increasing slightly from 51.56% to 55.56% as the laser intensity rises.

The physical origin for the RIET-type back-to-back emission is revealed by the typical trajectory illustrated in Figs. 2(c) and 2(f). Here, the outer electron born in the $-z$ direction nearly at positive maximum field is thrown back to recollide with the inner electron at about 0.7 o.c., slightly before a field zero. After the recollision, the returned electron with positive energy runs to the $+z$ direction for a while, driven by the instantaneous negative field, but the field soon becomes positive and hence forces the returned electron to reverse its direction and emit in the $-z$ direction. On the other hand, the inner electron is excited after the recollision, waiting until the next peak field arrives. At that time, the Coulomb barrier is dramatically suppressed and the electron can be released through quantum tunneling, as evidenced by the energy jump [29] at $t \simeq 1.0$ o.c.. However, the excitation-tunneled electron could not be accelerated away from the nucleus, since it does not ionize until $t \simeq 1.45$ o.c., that is, after an additional half-cycle time delay. The reason is as follows. The electron tunneled slightly before the maximum of the laser field is only quasi-free (i.e., a long distance from the nucleus but with negative energy). As soon as the external field decreases, the electron feels the nuclear field, hindering the electron to be driven away. When the field reverses, however, it is effectively driven toward the nucleus and through a phase

shift induced by electron-nucleus scattering it can now extract enough energy from the external field to escape. Here we notice the crucial role of the nuclear Coulomb attraction in the post-tunneling process. Without the nuclear attraction, according to the well-known simple-man model, we know that the electron tunneled before the field maximum would directly emit without returning to the core while the electron tunneled after the field maximum would return to the nucleus and then emit in the opposite direction in which it tunneled. The former gives the correlation while the latter leads to anticorrelation. These two processes are equally likely because the field in cosine form is symmetric with respect to its maximum. Nevertheless, the nuclear Coulomb attraction effect will break the balance by increasing the possibility of the latter process, which favors the anticorrelation. This has been evidenced by our calculation shown in Figs. 2(c) and 2(f), in which the electron tunneled slightly before the field maximum still returns to the nucleus and then emits in the opposite direction in which it tunneled.

The time over which the inner electron populates the excited state prolongs as the laser intensity decreases. For a very long time delay, both same-hemisphere and opposite-hemisphere emissions are possible and become equally important. Thus, there is no significant signal of anticorrelation at very low laser intensity, as shown in the bottom-right plot of Fig. 1.

According to this analysis, an interesting picture for the RIET-induced back-to-back emission emerges as follows: (i) The outer electron born in the $-z$ direction is thrown back by the field to recollide with the inner electron. After that, the returned electron is driven by the field to run to the $+z$ direction for a while, reverse its direction, and finally emit in the $-z$ direction. (ii) The recollision-excited electron tunnels out of the Coulomb barrier in the $-z$ direction. The electron feels the nuclear Coulomb attraction, which hinders the electron from being driven away. It waits for a half-cycle so that the laser field reverses its direction and drives it back to the nucleus. The electron finally emits in the $+z$ direction. This picture is different from the mechanism discussed in Ref. [9] where the escape of the excited electron at the first field maximum after recollision is hindered by the proximity of the other electron.

Based on these calculations and discussion, the physical picture for the double ionization at the transition to the BRT regime is summarized in the percentile map of Fig. 3. Our results unveil that (i) both the mechanisms of RIDI and RIET significantly contribute to the double ionization yield; (ii) the RIDI mechanism plays a decisive role in the transition from correlation to anticorrelation; and (iii) the RIET mechanism always prefers to cause back-to-back emission. Its percentage over the total NSDI events increases monotonically as the laser intensity decreases.

Another signature for the transition to the BRT regime, as we have pointed out, is the disappearance of the striking V-shaped structure in the correlated momentum spectra. Above the threshold, the V-shaped structure is shown to be closely related to the relative perpendicular momentum between two electrons (see Fig. 3 of Ref. [20]). The question is how the anticorrelated pattern concerned in this paper depends on the relative perpendicular momentum. To answer it, we make some further calculations. We first show the distribution of the relative perpendicular momentum p_{12}^{\perp} for all DI events in

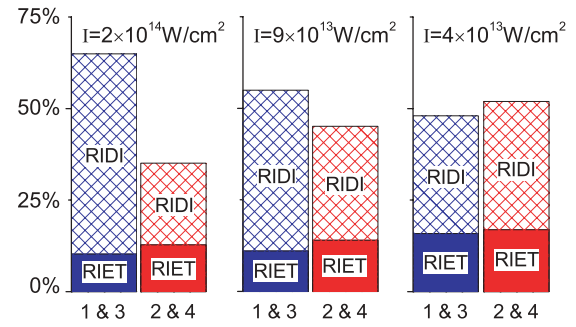


FIG. 3. (Color online) Percentile map for doubly ionizing trajectories at three different laser intensities. All trajectories are classified into two categories based on whether the inner electron is freed through RIDI (hatched area) or RIET (color-filled area). The numbers at the bottom denote the quadrants of the correlated momentum plane.

Fig. 4(d). It can be divided into three regimes: a rapid ascent, followed by a cambered top around $p_{12}^{\perp} = 0.4$ a.u., and finally a gentle slope. The correlated parallel momentum spectra for these three different regimes are, respectively, shown in Figs. 4(a)–4(c). We find that those electron pairs with small relative perpendicular momentum are mainly responsible for the anticorrelation. As p_{12}^{\perp} increases, the distribution becomes uniform, occupying four quadrants, and finally the well-known correlated pattern emerges.

This calculation indicates that, if the electrons are emitted with small relative transverse momentum, then they are most likely found to be anticorrelated. In these DI events, we have found that both electrons emit almost along the polarization axis (i.e., their transverse momentum are also small). This indicates the important role of $e-e$ Coulomb repulsion in forming the anticorrelation pattern, because the Coulomb

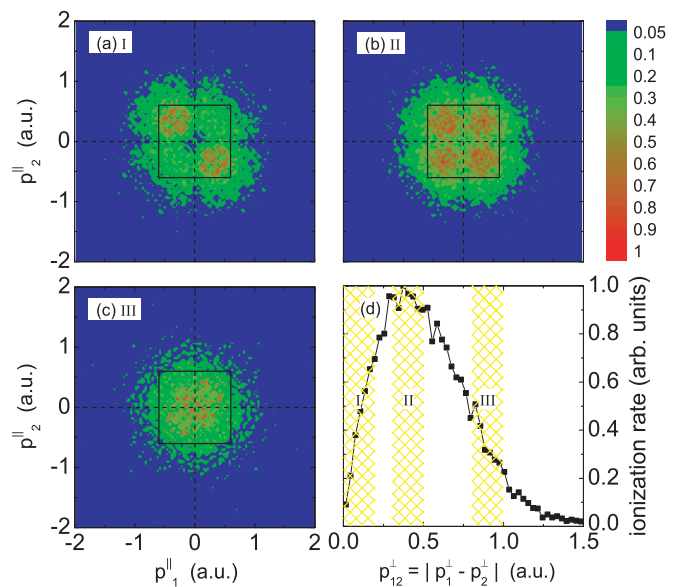


FIG. 4. (Color online) Correlated parallel momentum distributions with additional conditions on the relative perpendicular momentum between two electrons: (a) $0 \leq p_{12}^{\perp} \leq 0.2$, (b) $0.3 \leq p_{12}^{\perp} \leq 0.5$, and (c) $0.8 \leq p_{12}^{\perp} \leq 1.0$. (d) The overall relative perpendicular momentum distribution. The laser intensity is 4×10^{13} W/cm².

repulsion is strongly enhanced if the electrons with small transverse momenta are selected. This observation is consistent with our previous discussion. We suggest future experiments to verify this prediction.

B. Discussion on the threshold intensity

As demonstrated in the previous section, our semiclassical model, which includes recollision-induced excitation tunneling but without considering the shielding effect and multiphoton processes, has captured the key feature of the double ionization at the transition to the BRT regime. Our model calculation clearly indicates that the threshold value is shifted downward in comparison with the simple criterion $3.17U_p = |I_{p2}|$. This point has been claimed theoretically in previous works [30,31].

The underlying mechanism can be uncovered by the typical double ionization trajectories represented by Fig. 2(a) and 2(d). We see that, due to the field suppression of the Coulomb potential, electrons with negative energy can still escape from the atom as long as their energy is higher than the maximal barrier height. A quantitative estimation of the field suppression effect has been made using a simple 1D model [30]: Because the maximum of the barrier in the 1D potential $V(z) = -2/|z| + \epsilon_0 z$ ($z < 0$) is given by $V_b = -2\sqrt{2\epsilon_0}$, an incoming electron with kinetic energy E_{kin} has sufficient energy to eject a second electron when $-|I_{p2}| + E_{\text{kin}} > 2V_b = -4\sqrt{2\epsilon_0}$. It is then expected that this formula should give the correct threshold intensity by replacing E_{kin} with the maximum kinetic energy of the incoming electron $3.17U_p$ [30].

However, the barrier height varies with the angle to the polarization axis (e.g., the barrier in other directions will be higher). To include this lateral effect, we need to consider the full 3D Schrödinger equation of an atom in a uniform field. Using atomic units and taking the nuclear charge to be two, we then have $(\frac{1}{2}\nabla^2 + E + \frac{2}{r} - \epsilon_0 z)\psi = 0$ [32]. This allows separation of the variables in parabolic coordinates: $\xi = r + z$, $\eta = r - z$, $\varphi = \arctan(y/x)$, and the eigen wave function is of the form $\psi = \frac{\chi_1(\xi)\chi_2(\eta)}{\sqrt{\xi\eta}}$. Variable separation leads to two equations: $\frac{1}{2}\frac{d^2\chi_1}{d\xi^2} + [\frac{E}{4} - U_1(\xi)]\chi_1 = 0$ and $\frac{1}{2}\frac{d^2\chi_2}{d\eta^2} + [\frac{E}{4} - U_2(\eta)]\chi_2 = 0$. Each of the equations takes the form of a 1D Schrödinger equation, where the effective energy is $E/4$ and the effective potentials take the form $U_1(\xi) = -\frac{\beta_1}{2\xi} - \frac{1}{8\xi^2} + \frac{\epsilon_0\xi}{8}$ and $U_2(\eta) = -\frac{\beta_2}{2\eta} - \frac{1}{8\eta^2} - \frac{\epsilon_0\eta}{8}$, respectively. Note that the separation constants fulfill $\beta_1 + \beta_2 = 2$, which equals the nuclear charge. Along the ξ coordinate the state is bounded while there exists a potential barrier along the η coordinate; the ionization of the electron from the atom in the direction $z \rightarrow -\infty$ corresponds to its passage into the region of large η . Approximately we take $\beta_1 = \beta_2 = 1$ [33]. The maximum of the barrier is estimated to be $V_b \simeq -\sqrt{\epsilon_0}/2$.

On the other side, after the recollision, the kinetic energy of the returned electron will be shared by the struck one (i.e., $E_r + E_s \simeq 3.17U_p - |I_{p2}|$, where E_r and E_s denote the energy of returned electron and struck electron after recollision, respectively). Thus, single-recollision-induced DI becomes possible only when both electrons can pass over the suppressed barrier [i.e., $\min(E_r/4, E_s/4) \geq V_b$]. Obviously, the solution of this inequality depends on how the energy is

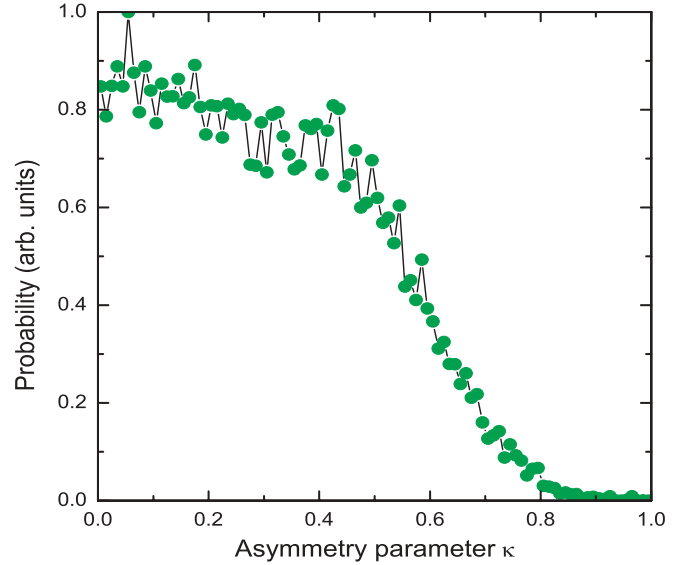


FIG. 5. (Color online) Statistics on distribution probability with respect to the asymmetry parameter. The trajectories with the maximum returned energy $\simeq 3.17U_p$ are selected out to calculate the energy apportion after recollision. The laser parameters are 7×10^{13} W/cm² and 800 nm.

shared by the electrons after recollision. We thus introduce the asymmetry parameter $\kappa = |(E_r - E_s)/(E_r + E_s)|$ to characterize the energy apportion. We consider the regime that $3.17U_p - |I_{p2}| < 0$ and both electrons populate bound states after the recollision. $\kappa = 0$ corresponds to equal energy sharing while $\kappa = 1$ corresponds to the most uneven energy apportion. For a given κ , the threshold intensity will be determined through following equation:

$$3.17U_p - |I_{p2}| \simeq -4/(1 + \kappa)\sqrt{\epsilon_0}, \quad 0 \leq \kappa \leq 1. \quad (2)$$

In practice, the energy is usually not equally allotted to the returned electron and struck electron after recollision. Numerically, we have compiled statistics on the distribution probability with respect to the asymmetry parameter κ in Fig. 5, where the parameters are chosen close to the threshold. It shows that the distribution function has a broad peak around zero with a long tail and decreases to zero at $\kappa = 1$. According to our calculation, the main profile of the distribution function is general while some detailed structures vary with the field parameters and the atomic structure.

In general, Eq. (2) defines a narrow transition zone whose upper boundary corresponds to $\kappa = 1$ and lower boundary corresponds to $\kappa = 0$ in the plot of intensity versus wavelength as shown in Fig. 6. Above the zone, the DI events are mainly induced by single recollision and therefore the side-by-side emission dominates, whereas, below the zone, single-recollision-induced DI is forbidden and the anticorrelation becomes prominent. The transition from correlation to anticorrelation is expected to emerge in the transition zone.

For practical application, we simplify our discussion by taking a simple algebraic average of the prefactor on the right-hand of Eq. (2) for the two limiting cases $\kappa = 0$ and 1; this gives an approximate threshold field through the following

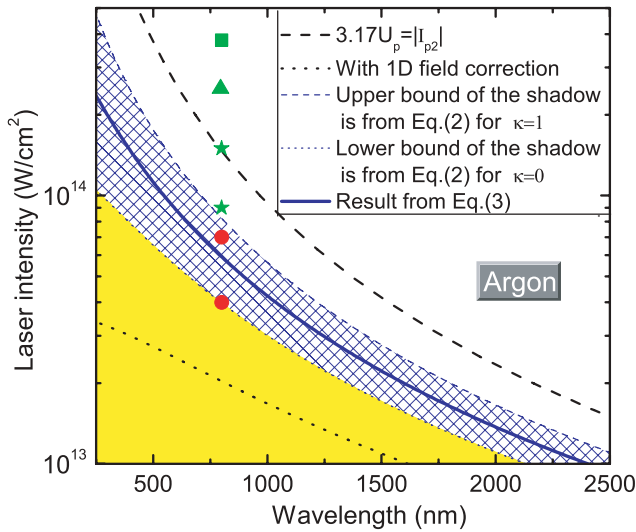


FIG. 6. (Color online) Threshold intensity vs laser wavelength. Comparisons are made between various theories and experimental data taken from the literature: Ref. [5] (■), Ref. [34] (▲), Ref. [31] (★), and Ref. [8] (●). Green (light gray) and red (dark gray) indicate that the observed pattern is correlation and anticorrelation, respectively.

self-consistent equation:

$$3.17 \left(\frac{\epsilon_{\text{th}}^2}{4\omega^2} \right) - |I_{p2}| \simeq -3\sqrt{\epsilon_{\text{th}}}. \quad (3)$$

The threshold field ϵ_{th} could approximately demarcate the transition from correlation-dominated emission to a regime where anticorrelation plays an important and finally even dominant role. It is independent of the asymmetry parameter κ , and therefore it is general and feasible for the DI analysis of other helium-like atoms.

Our theory has been compared with existing data as shown in Fig. 6. Obviously, our theory is consistent with the experimental data to a large extent, while the simple criterion $3.17U_p = |I_{p2}|$ overestimates the threshold and the model with 1D field correction underestimates the threshold.

IV. DISCUSSION AND CONCLUSION

Nonsequential double ionization below the recollision threshold has attracted considerable attention during the past few years. In several experiments claims were made that this intriguing regime had been reached [18,31,35,36]; however, the dominance of back-to-back emission was not observed. That is because, according to our present understanding,

the laser intensities used did not penetrate into the BRT regime, whose boundary had shifted downward to a lower intensity regime due to the field suppression effect. This is also the reason why quantum calculations made by directly solving the Schrödinger equations also did not reveal any apparent anticorrelation [10,18]. On the other hand, from a first intuitive glance, it is believed that BRT is a situation where classical considerations no longer hold [8]. However, a recent purely classical calculation did reproduce the observed feature of anticorrelation [9]. This raises a controversy as to whether the anticorrelation is caused by an effect that is inherent to quantum mechanics or can be captured by classical mechanics as well. The contradiction is eliminated by the quantitative calculations carried out by our semiclassical model that involves both the quantum effect and classical rescattering. We show that both the RIET (mainly quantum) and RIDI (mainly classical) mechanisms contribute to the NSDI at the transition to the BRT regime and that the latter is more important, contributing more than two-thirds to the total DI events. On the other hand, our calculations on the RIET mechanism contradict the simple picture proposed in Ref. [34], in which it is claimed that NSDI events caused by RIET should be averagely distributed among the four quadrants.

In conclusion, we have investigated the strong-field double ionization at the transition to below the recollision threshold using a semiclassical approach. It is found that the two-electron momentum distribution changes from correlation to anticorrelation and the V-shaped structure in the correlated momentum spectra fades away. Both RIET and multiple recollisions are responsible for the transition and are found to leave distinct footprints on the correlated momentum spectra. In addition, our model calculations reveal that the striking anticorrelation phenomenon is closely related to the relative perpendicular momentum distribution: Those electron pairs with small relative perpendicular momentum are mainly responsible for the anticorrelation. On the other hand, we claim that the appearance of the anticorrelated pattern signals the transition to the BRT regime. Discussion of the threshold intensity is made.

ACKNOWLEDGMENTS

We thank J. Ullrich and Yunquan Liu for helpful discussions. This work is supported by the National Fundamental Research Programme of China (Contact Nos. 2007CB814800 and 2007CB815103), the National Natural Science Foundation of China (Contact No. 10725521), and the Foundation of CAEP (Contact No. 2006Z0202).

- [1] B. Walker, B. Sheehy, L. F. Dimauro, P. Agostini, K. J. Schafer, and K. C. Kulander, *Phys. Rev. Lett.* **73**, 1227 (1994).
 [2] D. N. Fittinghoff, P. R. Bolton, B. Chang, and K. C. Kulander, *Phys. Rev. Lett.* **69**, 2642 (1992).
 [3] P. B. Corkum, *Phys. Rev. Lett.* **71**, 1994 (1993).
 [4] U. Eichmann, M. Dörr, H. Maeda, W. Becker, and W. Sandner, *Phys. Rev. Lett.* **84**, 3550 (2000).

- [5] Th. Weber *et al.*, *Nature (London)* **405**, 658 (2000).
 [6] Th. Weber *et al.*, *Phys. Rev. Lett.* **84**, 443 (2000); R. Moshhammer *et al.*, *ibid.* **84**, 447 (2000).
 [7] A. Staudte *et al.*, *Phys. Rev. Lett.* **99**, 263002 (2007); A. Rudenkov *et al.*, *ibid.* **99**, 263003 (2007).
 [8] Y. Liu *et al.*, *Phys. Rev. Lett.* **101**, 053001 (2008).
 [9] S. L. Haan, Z. S. Smith, K. N. Shomsky, and P. W. Plantinga, *J. Phys. B* **41**, 211002 (2008).

- [10] D. I. Bondar, W.-K. Liu, and M. Yu. Ivanov, *Phys. Rev. A* **79**, 023417 (2009).
- [11] M. V. Ammosov, N. B. Delone, and V. P. Krainov, *Zh. Eksp. Teor. Fiz.* **91**, 2008 (1986) [*Sov. Phys. JETP* **64**, 1191 (1986)].
- [12] L.-B. Fu, J. Liu, J. Chen, and S.-G. Chen, *Phys. Rev. A* **63**, 043416 (2001); L.-B. Fu, J. Liu, and S.-G. Chen, *ibid.* **65**, 021406(R) (2002).
- [13] R. Abrines and I. C. Percival, *Proc. Phys. Soc. London* **88**, 861 (1966); J. G. Leopold and I. C. Percival, *J. Phys. B* **12**, 709 (1979).
- [14] J. S. Cohen, *Phys. Rev. A* **64**, 043412 (2001); K. I. Dimitriou, D. G. Arbó, S. Yoshida, E. Persson, and J. Burgdörfer, *ibid.* **70**, 061401(R) (2004).
- [15] R. H. Garvey, C. H. Jackman, and A. E. S. Green, *Phys. Rev. A* **12**, 1144 (1975).
- [16] L. V. Keldysh, *Sov. Phys. JETP* **20**, 1307 (1965).
- [17] Y. Zhou, Q. Liao, and P. Lu, *Phys. Rev. A* **80**, 023412 (2009).
- [18] J. S. Parker, B. J. S. Doherty, K. T. Taylor, K. D. Schultz, C. I. Blaga, and L. F. DiMauro, *Phys. Rev. Lett.* **96**, 133001 (2006).
- [19] J. S. Prauzner-Bechcicki, K. Sacha, B. Eckhardt, and J. Zakrzewski, *Phys. Rev. Lett.* **98**, 203002 (2007).
- [20] D. F. Ye, X. Liu, and J. Liu, *Phys. Rev. Lett.* **101**, 233003 (2008).
- [21] S. L. Haan, J. S. Van Dyke, and Z. S. Smith, *Phys. Rev. Lett.* **101**, 113001 (2008).
- [22] A. Emmanouilidou, *Phys. Rev. A* **78**, 023411 (2008).
- [23] Here, we do not include the interaction with the laser field in energy and require energy greater than zero for an electron to be considered ionized, analogously to many others, e.g., S. L. Haan, L. Breen, A. Karim, and J. H. Eberly, *Phys. Rev. Lett.* **97**, 103008 (2006); S. L. Haan and Z. S. Smith, *Phys. Rev. A* **76**, 053412 (2007).
- [24] J. Liu, D. F. Ye, J. Chen, and X. Liu, *Phys. Rev. Lett.* **99**, 013003 (2007); see also D. F. Ye, J. Chen, and J. Liu, *Phys. Rev. A* **77**, 013403 (2008), for more details.
- [25] B. Hu, J. Liu, and S.-G. Chen, *Phys. Lett. A* **236**, 533 (1997).
- [26] K. N. Shomsky, Z. S. Smith, and S. L. Haan, *Phys. Rev. A* **79**, 061402(R) (2009).
- [27] F. Mauger, C. Chandre, and T. Uzer, *Phys. Rev. Lett.* **104**, 043005 (2010).
- [28] Because of the complexity of the DI dynamics in the BRT regime, sometimes there are many time moments when the energy of one electron becomes positive as demonstrated in Fig. 2(b). In this case, the ionization time is defined as the moment when the electron's energy turns from negative to positive and no longer returns to negative. A detailed statistical analysis according to the newly defined "time delay" will be presented in a forthcoming paper.
- [29] The energy shown in Fig. 2 is the sum of kinetic energy and electron-nuclear Coulomb energy. It does not include the electron-field interaction energy. Thus, there exists an energy jump ($\simeq |\epsilon(t)[z_i^{\text{out}} - z_i^{\text{in}}]|$) when the electron tunnels out of the Coulomb barrier. If we include the interaction energy, the total electron energy should be conserved during the tunneling process.
- [30] H. W. van der Hart and K. Burnett, *Phys. Rev. A* **62**, 013407 (2000).
- [31] E. Eremina *et al.*, *J. Phys. B* **36**, 3269 (2003).
- [32] L. D. Landau and E. M. Lifshitz, *Quantum Mechanics* (Pergamon Press, New York, 1977).
- [33] In analogy to the discussion in p. 293 of *Quantum Mechanics* by D. Landau and E. M. Lifshitz (Pergamon Press, New York, 1977), the dependence of wave function ψ on variable ξ can be regarded as being of the same form as that when the external field is absent. It gives $\beta_1 = \beta_2 = 1$.
- [34] B. Feuerstein *et al.*, *Phys. Rev. Lett.* **87**, 043003 (2001).
- [35] M. Weckenbrock *et al.*, *Phys. Rev. Lett.* **92**, 213002 (2004).
- [36] D. Zeidler, A. Staudte, A. B. Bardon, D. M. Villeneuve, R. Dorner, and P. B. Corkum, *Phys. Rev. Lett.* **95**, 203003 (2005).